The effect of accelerated cooling on the structure of pipe steels for thermomechanical controlled processing

Cite as: AIP Conference Proceedings **2053**, 030029 (2018); https://doi.org/10.1063/1.5084390
Published Online: 19 December 2018

M. L. Krasnov, S. I. Platov, V. N. Urtsev, S. V. Danilov, V. I. Pastukhov, and M. L. Lobanov

The Effect of Accelerated Cooling on the Structure of Pipe Steels for Thermomechanical Controlled Processing

M. L. Krasnov[1, a)], S. I. Platov[2, b)], V. N. Urtsev[3, c)], S. V. Danilov[4, d)], V. I. Pastukhov[4,5, e)], and M. L. Lobanov[4, f)]

[1]*Magnitogorsk Iron and Steel Works OJSC, 93 Kirova St., Magnitogorsk, 455000, Russia.*
[2]*Nosov Magnitogorsk State Technical University, 38 Lenina Ave., Magnitogorsk, 455000, Russia.*
[3]*Ausferr Research and Technology Center, 18 Gorkogo St., Magnitogorsk, 455000, Russia.*
[4]*Ural Federal University, 19 Mira St., Ekaterinburg, 620002, Russia.*
[5]*Institute of Nuclear Materials JSC, PO Box 29, Zarechny, Sverdlovsk Region, 624250, Russia.*

[a)]krasnov.ml@mmk.ru
[b)]psipsi@mail.ru
[c)]urtsev@inbox.ru
[d)]Corresponding author: s.v.danilov@bk.ru
[e)]vladimir.pastuhov@urfu.ru
[f)]m.l.lobanov@urfu.ru

Abstract. Scanning electron microscopy with orientation analysis by the electron backscatter diffraction (EBSD) method is used to study microstructures and textures formed in low-carbon low-alloy pipe steel after thermomechanical controlled processing (TMCP) and subsequent quenching with cooling rates of 50 to 700 °/s. It has been established that, in the range of industrial rates of cooling between 50 and 350 °/s from austenitic regions, the γ→α transformation starts at temperatures of 700–670 ºC and proceeds by the shear mechanism. As a result, a bainite structure of different dispersity with martensitic inclusions is predominantly formed.

INTRODUCTION

Increasing the operating pressure due to the use of highly resistant steels fit for operation under harsh climate conditions is one of the most promising ways of increasing the economic efficiency of trunk pipelines [1–3]. Highly resistant pipes are preferential due to reduced specific quantity of metal [2, 4, 5]. In mid-1970s the structural strength of low-alloy pipe steels of strength classes from X52–X65 to X70–X80 and further to X100 significantly increased due to development and industrial implementation of Thermomechanical Controlled Processing (TMCP) combining controlled rolling and subsequent accelerated controlled cooling [1, 2, 5–8]. High-strength classes were obtained due to a changeover from ferritic-pearlitic structures to shear transformation products – predominantly, bainite. Consistent acquisition of the latter was provided due to the control of the stability of supercooled austenite by alloying and application of controlled accelerated cooling [1, 2, 9–11].

The paper studies common patterns of structure formation in low-carbon low-alloy steel under accelerated cooling when the γ→α shear transformation occurs.

RESEARCH METHODS

The materials to be studied were samples cut out of industrial sheet of low-carbon low-alloy pipe steel (~0.05 wt% C, ≤2.0 wt% Mn, ~0.2 wt% Mo, ~0.05 wt% Nb, the rest being represented by iron and unavoidable

Mechanics, Resource and Diagnostics of Materials and Structures (MRDMS-2018)
AIP Conf. Proc. 2053, 030029-1–030029-4; https://doi.org/10.1063/1.5084390
Published by AIP Publishing. 978-0-7354-1781-6/$30.00

impurities), designed for production of large-diameter pipes of the X80 strength class. The samples had the form of 20×70 mm plates with thickness ranging between 0.25 and 1.10 mm.

Different sample cooling rates, including those reproducing technological parameters of production processing, were simulated on a unique facility, developed by the Ausferr Research and Technology Center, consisting of a reheating furnace with a sample removal and fixation mechanism, a temperature measuring unit, an air cooling unit with a pneumatic system, control and information recording unit.

The samples were heated in the furnace to an austenization temperature of 980 °C, and then cooled for 30 minutes. The sample cooling rate was controlled by sample thickness and air cooling pressure. As a result, a set of samples cooled at temperatures ranging between 980 °C and effective temperature for phase transition t_0 with rates ($V_C = dT/d\tau$) ranging from 50 to 700 °/s was obtained.

An electron microscopic study of the structure was carried out using a Tescan Mira3 scanning microscope with a field emission cathode at an accelerating voltage of 20 kV (Fig. 1). An EBSD HKL Inca attachment with an Oxford Instruments analysis system was used to determine the orientations of individual grains and to analyze the local structure. The scanning interval was 0.1 μm. An error of lattice orientation determination did not exceed ±1° (±0.6° on average). Low-angle boundaries between local volumes were built on orientation maps for disorientation from 1 to 6° (1 pixel thick lines), high-angle boundaries being mapped for disorientations not exceeding 15° (3 pixel thick lines), Fig. 1g, h, i. High accuracy of orientation determination and, as a consequence, that of local disorientations during EBSD-analysis (more than 95% recognition for all the studied areas) allowed using Oxford Instruments software to determine the average crystallite size (D_{av}). As a crystallite, an object limited on every side by boundaries with disorientation angles of at least 15° was taken.

RESULTS AND DISCUSSION

Thermogram analysis $t = f(\tau)$ has shown that, at cooling rates of 50 to 450 °/s, the γ→α transformation starts at temperatures of 700–670 ºC. Moreover, the most part of the transition occurs under conditions close to isothermal. It corresponds to the decay of supercooled austenite by the diffusive mechanism.

In case of a high cooling rate (V_C = 693 °/s), a structure characteristic of martensite package (Fig. 1a, d, g), consisting of alternating rods D_{av} = 0.97±0.03 μm was observed. A decrease in V_C to 449 °/s caused the formation of a significantly less uniform structure, where, along with martensite packages, larger individual (out-of-package) crystallites characterized by nonequilibrium forms, sized up to 20 μm at D_{av} = 1.2±0.1 μm, were detected. At V_C equal to 202 and 166 °/s, martensite packages almost disappeared from the structure. The structure was represented by non-equiaxial irregularly shaped crystallites sized up to 20 μm, with small dark inclusions on their boundaries (Fig. 1b, e, h). With higher magnification, it was obvious that these inclusions were not precipitations and that they were determined by their own substructure, close to the package one. D_{av} were 1.5±0.1 and 1.7±0.1 μm, respectively. At further cooling deceleration to 110 °/s and below, the crystallite forms of the main structure became more equiaxial (Fig. 1c, f, i) at D_{av} = 2.0±0.2 μm. The crystallite boundaries tended to straighten. The volume fraction and size of dark inclusions increased. Orientation microscopy allows claiming that the inclusions represent martensite packages, where carbon-enriched austenite decays last.

In case of sample cooling in the whole V_C range, the spectra of intercrystalline boundaries corresponded to the structures resulting from shear transformations (Fig. 2) [12, 13]. All epy high-angle boundaries were concentrated in disorientation angles ranging between 49 and 60º (Fig. 2a, b, c). In special boundary spectra, predominantly CSL boundaries were registered – Σ3, Σ11, Σ25b, Σ33c, and Σ41c (Fig. 2d, e, f). It was shown in [12] that this spectrum is caused by shear phase transition according to orientation relationships (OR) intermediate between the Kurdyumov-Sachs and Nishiyama-Wassermann OR.

CONCLUSION

It has been established that, in low-carbon low-alloy steel for TMCP under cooling rates ranging between 50 and 450 °/s from austenitic regions, the γ→α transformation starts at temperatures of 700–670 ºC and proceeds by the shear mechanism. As a result, a bainite structure of different dispersity with martensitic inclusions is predominantly formed. As the cooling rate increases, the bainite grain size nearly halves, while size and volume fraction of martensite inclusions increases.

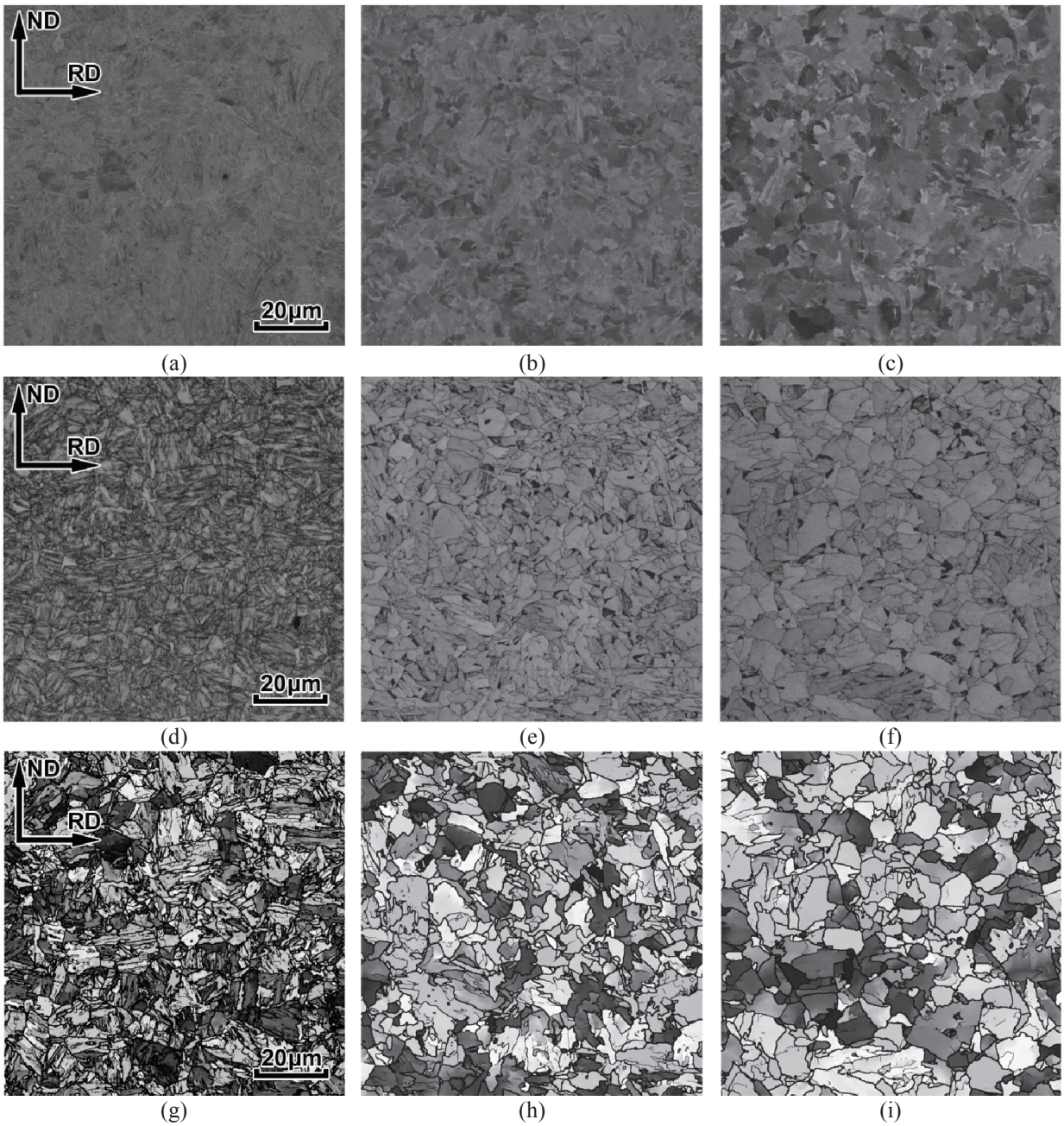

FIGURE 1. Microstructures in reflected (a, b, c), backscattered (d, e, f) electrons and in the form of EBSD orientation maps with intercrystalline boundaries (g, h, i); a, d, g – V_C = 693 °/s; b, e, h – 166 °/s; c, f, i – 110 °/s

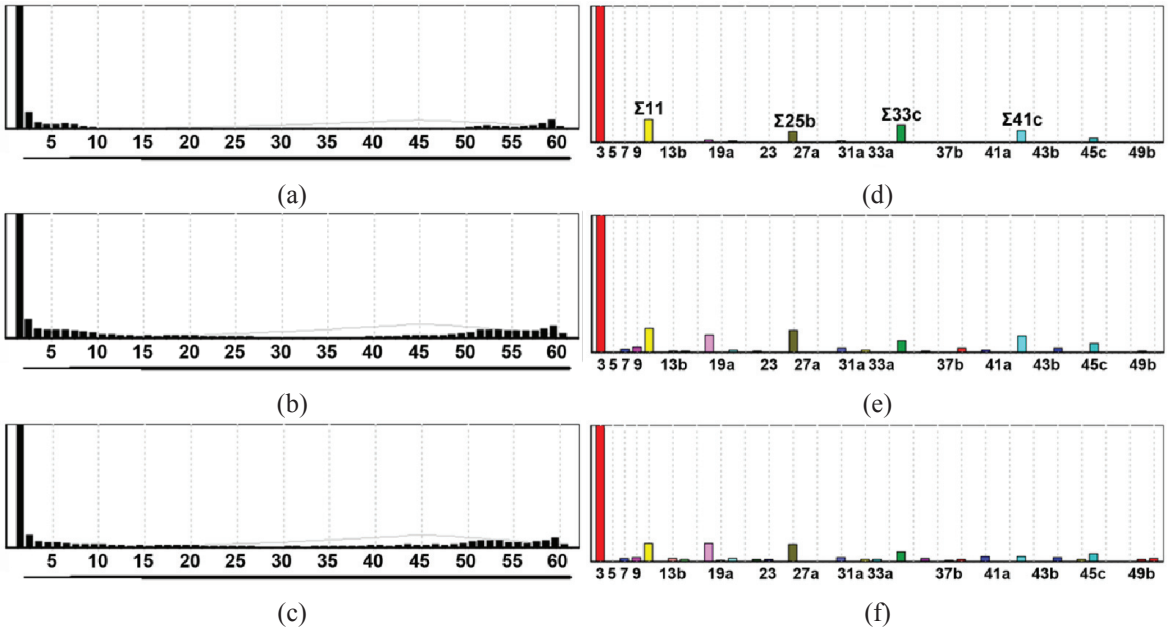

FIGURE 2. Intercrystalline (a, b, c) and CSL (d, e, f) boundary spectra at different cooling rates; a, d – V_C = 693 °/s; b, e – 166 °/s; c, f – 110 °/s

ACKNOWLEDGMENTS

The work was done using the equipment of the Laboratory of Structural Methods of Analysis and Properties of Materials and Nanomaterials of the Collective Use Center affiliated to the B. N. Yeltsin Ural Federal University. The study was supported by the program for increasing the competitiveness of the leading Russian universities, RF Government resolution No. 211, contract No. 02.A03.21.0006.

REFERENCES

1. E. Shigeru and N. Naoki, JFE Technical Report. **20**, 1–7 (2015).
2. D. G. Stolheim, Metallurgist **55**, 53–66 (2013) (In Russ).
3. S. Y. Nastich, V. L. Kornilov, Y. D. Morozov, S. V. Denisov and M. A. Molostov, Steel in Translation **39**, 431–436 (2009).
4. M.-C. Zhao, K. Yang and Y. Shan, Materials Science and Engineering A **335**, 14–20 (2002).
5. K. Hulka, P. Peters and F. Haisterkamp, Stall **10**, 62–67 (1997) (In Russ).
6. M. Yu. Matrosov, A. A. Kichkina, A. A. Efimov, L. I. Éfron and O. A. Bagmet, Metallurgist **51**, 367–376 (2007).
7. A. B. Arabey, Steel in Translation **40**, 601–608 (2010).
8. I. Y. Pyshmintsev, A. O. Struin, A. M. Gervasyev, M. L. Lobanov, G. M. Rusakov, S. V. Danilov and A. B. Arabey, Metallurgist **60**, 405–412 (2016).
9. H. K. Sung, S. Y. Shin, B. Hwang, C. G. Lee, N. J. Kim and S. Lee, Materials Science and Engineering A **530**, Pages 530–538 (2011).
10. J. Cao, J. Yan, J. Zhang and T. Yu, Materials Science and Engineering A **639**, 192–197 (2015).
11. Z. J. Xie, X. P. Ma, C. J. Shang, X. M. Wang and S. V. Subramanian, Materials Science and Engineering A **641**, 37–44 (2015).
12. M. L. Lobanov, G. M. Rusakov, A. A. Redikul'tsev, S. V. Belikov, M. S. Karabanalov, E. R. Struina and A. M. Gervas'ev, Physics of Metals and Metallography **117**, 254–259 (2016).
13. M. L. Lobanov, M. D. Borodina, S. V. Danilov, I. Y. Pyshmintsev and A. O. Struin, Steel in Translation **47**, 710–716 (2017).